Desalination and Water Treatment
www.deswater.com
doi: 10.5004/dwt.2020.25845

194 (2020) 180–186
August

Preparation of amphoteric modified magnetized biochar and its adsorption of Cu(II)

Jia Xie[a], Hong-yan Deng[a], Lang Zhu[a], Yi-fang Zhang[a], Wen-bin Li[a,*], Dan Wang[a], Zhao-fu Meng[b]

[a]*College of Environmental Science and Engineering, China West Normal University, Nanchong, Sichuan 637009, China, Tel. +86 08172568455; emails: lwb062@163.com (W.-b. Li), 291961575@qq.com (J. Xie), dhongyan119@163.com (H.-y. Deng), 1994517604@qq.com (L. Zhu), 2656526319@qq.com (Y.-f. Zhang), 415965371@qq.com (D. Wang)*
[b]*Department of Natural Resource and Environment, Northwest A&F University, Yangling 712100, China, email: zfmeng@hotmail.com (Z.-f. Meng)*

Received 11 October 2019; Accepted 17 March 2020

ABSTRACT

Magnetized biochar (MB) was prepared by co-precipitation-supported Fe_3O_4 method to investigate the adsorption characteristics of Cu^{2+} in aqueous solution by amphoterically modified MB (MB_{BS}). MB was modified by dodecyl dimethyl betaine (BS-12) with modification ratios of 0%, 25%, 50%, 100%, 150%, and 200% cation exchange capacity (CEC) of MB for preparing MB, MB_{25BS}, MB_{50BS}, MB_{100BS}, MB_{150BS}, and MB_{200BS}, respectively. Basic physicochemical properties of different MB_{BS} materials were analyzed. Isothermal adsorption and thermodynamic characteristics of Cu^{2+} on different MB_{BS}s were studied by batch method, and the effects of pH, temperature, and ionic strength on Cu^{2+} adsorption were compared. Results showed the following. (1) The surface of biochar (B) loaded with Fe_3O_4 became rough, and that of MB modified by BS-12 became smooth gradually. The pH, CEC, and specific surface area of all MC_{BS} materials diminished with increased BS-12 modification ratio. (2) Adsorption isotherms of Cu^{2+} on different MB_{BS}s were L-shaped and accorded with Langmuir model. The maximum adsorption capacity of MB_{BS}s to Cu^{2+} ranged from 318.43 to 542.46 mmol/kg. The adsorption capacity of MB modified by BS-12 for Cu^{2+} was substantially enhanced compared with MB. (3) In the range of 20°C–40°C, the adsorption amount of Cu^{2+} on MB_{BS} materials all increased with the increase in temperature. The increase in pH was beneficial to the adsorption of Cu^{2+} by various MB_{BS} materials, whereas the increase in ionic strength inhibited the adsorption of Cu^{2+} by various MB_{BS}s. (4) Cu^{2+} adsorption by MC_{BS}s was a process of spontaneous, endothermic, and entropy increase.

Keywords: Amphoteric modification; Magnetination; Biochar; Cu^{2+}; Adsorption amount

1. Introduction

Heavy metals pollution in water progressively worsens due to the discharge of livestock raising, and industrial and agricultural wastewater [1–3], remediation, and treatment of this pollution has become an important concern [4–6]. Removal of heavy metal ions from wastewater by highly adsorptive materials is a simple, effective, and eco-environmental protection method, which bears significance for improving water environment and protecting human health [7,8].

Biochar (B) has the advantages of large specific surface area, strong adsorption capacity, and wide source of raw

* Corresponding author.

materials [9,10]. The high-efficiency adsorption of heavy metal ions also indicates the good application prospect of B [11–14]. Maximum adsorption capacities of green walnut peel B for Pb^{2+} and Cu^{2+} total 476.19 and 153.85 mg/g, respectively. The increase in temperature enhances the adsorption capacity of heavy metals [15], B exhibits a good adsorption capacity for various heavy metals [16]. B particles are small and can adsorb a large amount of pollutants. If pollutants are not separated in time, they would cause secondary pollution to the water body, which is also not conducive to the regeneration of B [17]. In recent years, several scholars have used co-precipitation method to magnetize B and formed magnetized B (MB) with good adsorption, magnetic separation, and regeneration properties [18,19]. In a study, the removal rates of Cd^{2+} and Zn^{2+} in wastewater by MB reached 50.6% and 49.1%, respectively. After five times of reuse, the adsorption rate of pollutants could still reach 76% [20]. Several scholars modified MB with chitosan, and the adsorption effect of the chitosan-modified MB on Cr^{6+} considerably increased, enabling researchers to further explore the adsorption capacity of MB for heavy metals. The maximum adsorption capacity of Cr^{6+} could reach 120 mg/g, which is four times that of the original B [21]. MB modified by iminodiacetic acid also exhibited a high adsorption capacity for Cd^{2+} (197.96 mg/g at 323 K) and retained the adsorption rate of 82.18% after five recycles [22]. The above results showed that the modified MB has stronger adsorption capacity and good regeneration performance for heavy metal ions.

An amphoteric surfactant features both positively and negatively charged hydrophilic groups and hydrophobic carbon chains. Materials modified by amphoteric surfactants can simultaneously adsorb organic compounds and heavy metal ions. Amphoteric surfactants possess good chemical stability, low irritation and toxicity, and environmentally feature [23]. Using amphoteric surfactants to modify clay minerals can effectively enhance their adsorption capacity to heavy metal cations [24]. Meng et al. [25] used dodecyl dimethyl betaine (BS-12)-modified Lou soil to adsorb Cd^{2+}, and the adsorption amount reached 1.3–1.8 times higher than that of unmodified soil. Therefore, secondary modification of MB with amphoteric surfactants not only enhances adsorption capacity of MB for heavy metals and organic pollutant but also achieves environmental friendliness and reusability. Currently, limited research considers this aspect. In this paper, BS-12 was selected to modify MB at modification ratios of 0%, 25%, 50%, 100%, 150%, and 200%. Basic physicochemical characteristics of amphoterically modified MBs (MB_{BS}) were analyzed. Adsorption characteristics of Cu^{2+} on MB with different amphoteric modification ratios were studied. In addition, the effects of temperature, pH, and ionic strength on Cu^{2+} adsorption were discussed to provide a theoretical basis for the study of heavy metal treatment from wastewater by amphoterictic MB.

2. Materials and methods

2.1. Materials

B, $FeCl_3·6H_2O$, and $FeSO_4·7H_2O$ were purchased from Chengdu Kelon Chemical Reagent Factory, Chengdu City, Sichuan Province, China.

BS-12, which provided by Xingguang Auxiliary Factory (Tianjin City, China), was used as the amphoteric modifier. Fig. 1 shows the structural formula of BS-12.

Cu^{2+} solution was used as the pollutant and prepared by using $CuSO_4·5H_2O$ (analytical reagent) purchased from Chengdu Kelon Chemical Reagent Factory.

2.2. Preparation of MB_{BS}

A co-precipitation method was used to prepare MB [26]. In this method, 20.00 g B was dispersed in 2.0 L distilled water (dH_2O) and stirred for 30 min. Under strictly anaerobic conditions, 0.4 M $FeCl_3·6H_2O$ and 0.2 M $FeSO_4·7H_2O$ were successively added to 60°C water, fully stirred for 2 h, and heated to 75°C. The pH was adjusted to 10 with 5 mol/L NaOH solution and the magnetic material was separated by magnets after continuous stirring for 1 h and natural cooling. MB could be obtained after washing several times with dH_2O. MB was dried at 60°C and then passed through a 60-mesh sieve.

A wet process was used to prepare MB_{BS} [6]. In this process, 100 g MB was slowly added to 1.0 L dH_2O, and different ratios of BS-12, which were calculated in accordance with the cation exchange capacity (CEC) of MB, was added again. After stirring at 40°C for 3 h, the samples were separated by magnets. The MC_{BS}s were washed by dH_2O thrice and dried at 60°C. MB_{BS}s were dried at 60°C for 12 h and passed through a 60-mesh sieve. Next, 0%, 25%, 50%, 100%, 150%, and 200% CEC BS-12-modified MB were prepared and recorded as MB, MB_{25BS}, MB_{50BS}, MB_{100BS}, MB_{150BS}, and MB_{200BS}, respectively. The weight of BS-12 for a certain weight of MC can be obtained by using Eq. (1).

$$W = m \times \text{CEC} \times M \times 10^{-6} \times \frac{R}{b} \tag{1}$$

where W (g) refers to the weight of BS-12, m (g) refers the weight of MB that will be modified, CEC (mmol/kg) represents the CEC of MB, M (g/mol) is the molecular mass of BS-12, R stands for the modified proportion of BS-12, and b specifies the product content of BS-12 (mass fraction).

2.3. Experimental design

2.3.1. Material characterization

B, MB, MB_{25BS}, MB_{50BS}, MB_{100BS}, MB_{150BS}, and MB_{200BS} (seven samples in total) were measured for CEC, specific surface area, and pH. Four representative samples of B, MB, MB_{50BS}, and MB_{100BS} were analyzed by scanning electron microscopy (SEM).

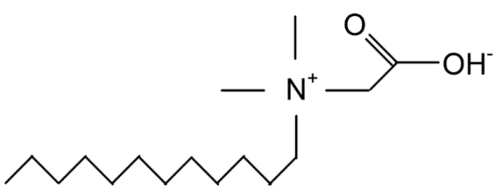

Fig. 1. Structural formula of BS-12.

2.3.2. Cu^{2+} concentration gradient

The preliminary experiment showed that the adsorption isotherm changed when the concentration reached 300–400 mg/L. Therefore, the concentration gradients of Cu^{2+} were set at 0, 20, 50, 100, 150, 200, 300, 400, and 500 mg/L. Each treatment was repeated thrice. The temperature was 30°C, the pH was 4, and the ionic strength was 0.1 mol/L NaCl.

2.3.3. Influence of environmental factors

Three single-factor experiments were performed considering pH, ionic strength, and temperature.

The experimental temperatures were set to 20°C, 30°C, and 40°C (pH value of the initial solution: 4; ionic strength: 0.1 mol/L NaCl). The pH of the initial solution was set to 3, 4, and 5 (initial solution temperature: 30°C; ionic strength: 0.1 mol/L NaCl). The ionic strength of the initial solution was set to 0.01, 0.1 mol/L and 0.5 mol/L NaCl (initial solution temperature: 30°C; pH: 4).

2.4. Experimental method

2.4.1. Analysis of physicochemical properties

The pH was determined by pH meter (Hach HQ411D); sodium acetate-ammonium acetate method was used to determine the CEC of the samples. The specific surface area was determined by the Brunauer–Emmett–Teller method (Analyzer ASAP2400, Micromeritics Instrument Ltd., Shanghai). Hitachi S-4800 (Japan) SEM was used to analyze sample morphology.

2.4.2. Cu^{2+} adsorption experiment

Batch equilibrium method was used for Cu^{2+} adsorption. A total of 0.1000 g samples were weighed in nine 50 mL plastic centrifuge tubes, and 20.00 mL Cu^{2+} solution with different concentration gradients was added into the pipette under the conditions of at constant temperature of 30°C, 150 r/min, and 12 h oscillation (the preliminary kinetic experiments showed that adsorption equilibrium was reached after 12 h) [27]. The equilibrium adsorption of Cu^{2+} in the supernatant was determined by centrifugation at 4,800 r/min for 20 min, the equilibrium adsorption amount of Cu^{2+} was determined, and the equilibrium adsorption amount of each material was calculated by subtraction. The Cu^{2+} content was determined via flame atomic absorption spectrophotometry, and background absorption was corrected through the Zeeman effect.

2.5. Data processing

2.5.1. Calculation of equilibrium adsorption amount

The equilibrium adsorption amount was calculated using Eq. (2):

$$q = \frac{\left(C_0 - C_e\right)V}{m} \tag{2}$$

where C_0 (mmol/L) and C_e (mmol/L) are the initial and equilibrium concentrations of Cu^{2+} in the solution, respectively. V (mL) is the volume of Cu^{2+} solution added. m (g) is the weight of the tested material. q (mmol/kg) is the equilibrium adsorption amount of Cu^{2+} on the tested material.

2.5.2. Fitting of adsorption isotherms

The Langmuir isotherm was selected based on the adsorption isotherm trend [28], and the isothermal equation (Eq. (3)) is as follows:

$$q = \frac{q_m bc}{1 + bc} \tag{3}$$

where q refers to the equilibrium adsorption amount of Cu^{2+} for the test material, mmol/kg; c denotes the equilibrium concentration of Cu^{2+} in the solution, mmol/L; q_m indicates the maximum adsorption amount of Cu^{2+} on the different materials, mmol/kg; b represents the apparent equilibrium constant of the Cu^{2+} adsorption, which can be used to measure the affinity of adsorption.

2.5.3. Calculation of thermodynamic parameters

Parameter b in the Langmuir model is equivalent to the apparent adsorption constant of equilibrium constant, and the thermodynamic parameter calculated by $b = K$ or K_a is called the apparent thermodynamic parameters, Eqs. (4)–(6) are as follows [29]:

$$\Delta G = -RT\ln K \tag{4}$$

$$\Delta H = R\left(\frac{T_1 \times T_2}{T_2 - T_1}\right) \times \ln\left(\frac{K_a, T_2}{K_a, T_1}\right) \tag{5}$$

$$\Delta S = \frac{\Delta H - \Delta G}{T} \tag{6}$$

where $\Delta G°$ is the standard free energy change (kJ/mol), R is a constant (8.3145 J/mol K), T is the adsorption temperature (T_1 = 293.16 K, T_2 = 313.6 K), $\Delta H°$ is the enthalpy of adsorption process (kJ/mol), and $\Delta S°$ is the entropy change of adsorption process (J/mol K).

Curve Expert 1.4 fitting software was used in isothermal fitting, and SigmaPlot 10.0 software was adopted to improve data plotting.

3. Results and discussion

3.1. Physicochemical properties of the tested materials

Analysis of physicochemical properties of the tested materials (Table 1) showed that the pH, CEC, and specific surface area of MB gradually declined compared with those of B. The pH, CEC, and specific surface area of the MB_{BS} decreased with the increase in BS-12 modification ratio. BS-12 had a carboxyl hydrophilic group and ionized hydrogen ions, resulting in a decrease in pH. The coverage of the B surface by the long carbon chain of BS-12 was the main factor for the decrease in CEC and specific surface area. The SEM image of different materials in Fig. 2

shows that the surface of the B material was smooth and had a partial pore structure. When the B surface was loaded with Fe_3O_4, the MB surface became rough, a large number of Fe_3O_4 particles adhered to the surface of B, and several pores were filled with Fe_3O_4 particles, these results are the same as those of Ren et al. [26]. Compared with MB_{50BS}, surface roughness of MB was lower, and particle density was higher mainly because the hydrophobic long carbon chain of BS-12 could form an organic phase on the surface of MB [25], the Fe_3O_4 particles bonded together, decreasing the surface roughness. MB_{100BS} exhibited a lower surface roughness and smoother surface than MB_{50BS}, and this finding was due to increased organic modification of BS-12 on the surface of MB.

Table 1
Basic physicochemical characteristics of each test material

Test materials	pH values	CEC (mmol/kg)	Specific surface-areas (m^2/g)
B	9.15	176.20	1,368.33
MB	8.88	150.34	408.69
MB_{25BS}	8.24	105.32	310.42
MB_{50BS}	8.01	88.27	224.60
MB_{100BS}	7.25	66.21	100.80
MB_{150BS}	7.00	41.37	69.83
MB_{200BS}	6.82	35.20	48.22

3.2. Isothermal adsorption characteristics of Cu^{2+} on test materials

Fig. 3 shows that at 30°C, the adsorption amount of Cu^{2+} on each MC_{BS} materials increased with the increase in equilibrium concentration and reached saturation. The adsorption isotherms were L-shaped. At the same equilibrium concentration, the adsorption capacity showed a trend of $MB_{50BS} > MB_{25BS} > MB_{100BS} > MB_{150BS} > MB_{200BS} > B > MB$.

Table 2 shows the fitting results of the adsorption isotherm via the Langmuir model. The correlation coefficients of the fitting results reached an extremely significant level, indicating that the adsorption of Cu^{2+} by different materials

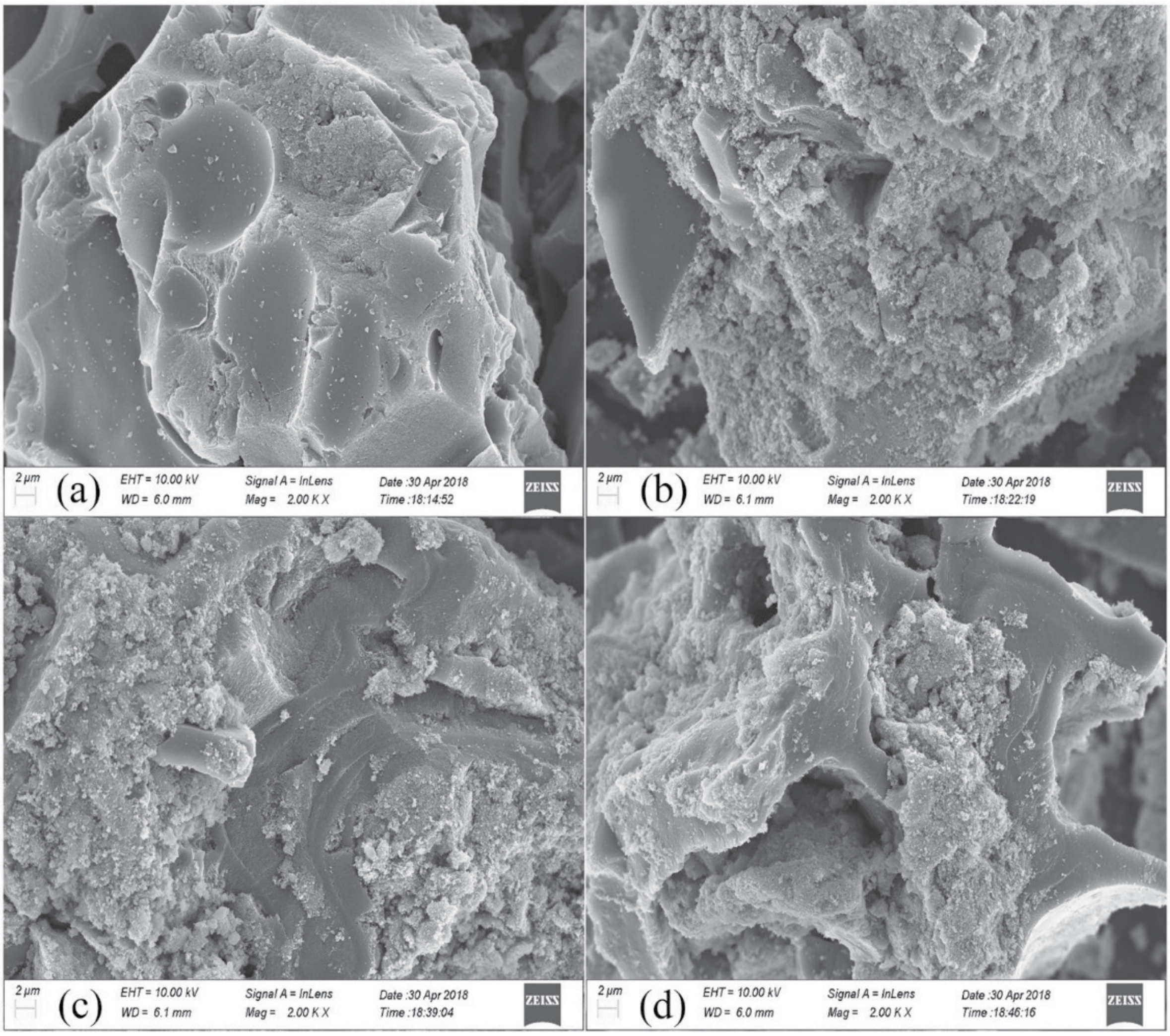

Fig. 2. SEM characteristics of B (a), MB (b), MB_{50BS} (c), and MB_{100BS} (d).

agreed with the Langmuir model. The maximum adsorption amount (q_m) was between 271.25 and 542.46 mmol/kg, and the ranking order was consistent with the adsorption capacity shown in Fig. 2. Compared with B, MB had a higher adsorption amount for Cu^{2+}. The Cu^{2+} q_m of MB_{BS} considerably increased and was 1.10–1.88 times higher than that of MB. The adsorption amount of Cu^{2+} on MB_{BS}s increased initially and then decreased with the increasing BS-12 modification ratio, the adsorption amount of MB_{50BS} for Cu^{2+} was the highest. Compared with the adsorption results of Cd^{2+} on amphoteric modified magnetic bentonites [30], the second modification of magnetic materials by BS-12 presented a main affinity toward heavy metals. The affinity constant b of each material for Cu^{2+} adsorption was maintained in the range of 0.26–0.38, showing consistency.

3.3. Effect of temperature and pH on Cu^{2+} adsorption

Fig. 4 shows the Cu^{2+} adsorption amount of all MB_{BS} materials under different temperatures. In the range of 20°C–40°C, the adsorption amount of Cu^{2+} increased with the increase in temperature, which indicated a positive temperature effect. The adsorption amount of Cu^{2+} on B increased by 6.76% from 20°C to 40°C, and that of Cu^{2+} by each MB_{BS} material increased by 6.78%–15.41%, The increase rate followed the order of MB_{50BS} (15.41%) > MB_{150BS} (12.64%) > MB_{25BS} (11.32%) > MB_{200BS} (10.87%) > MB (8.20%) > MB_{100BS} (6.78%). This result was mainly due to the ion exchange effect on Cu^{2+} by B, and complexation or chelation of Cu^{2+} by BS-12. The chemical exhibited an endothermic reaction and showed that increasing temperature was beneficial to the Cu^{2+} adsorption. This finding is consistent with Zhou's research results on Cd^{2+} adsorption [22].

The adsorption amount of Cu^{2+} on all materials increased in the range of pH 3–5. The adsorption amount of Cu^{2+} in

Table 2
Langmuir fitting parameters of Cu^{2+} adsorption by different materials

Test materials	Correlation coefficients/r	Standard deviations/S	q_m (mmol/kg)	b (L/mmol)
B	0.9978**	5.14	289.20	0.33
MB	0.9679**	16.92	271.25	0.26
MB_{25BS}	0.9942**	13.21	457.21	0.35
MB_{50BS}	0.9960**	11.99	542.46	0.29
MB_{100BS}	0.9819**	19.53	409.26	0.29
MB_{150BS}	0.9931**	10.79	323.94	0.38
MB_{200BS}	0.9952**	8.62	318.43	0.35

**indicates significance at the p = 0.01 level (r = 0.765 at p = 0.01 when the degrees of freedom f = 8).

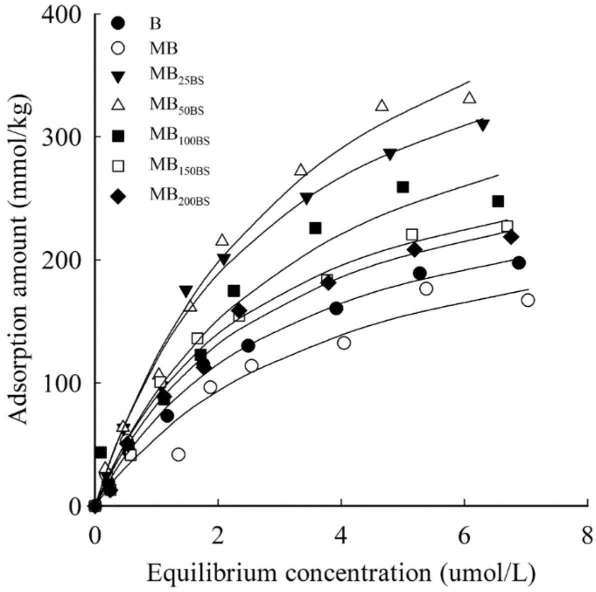

Fig. 3. Adsorption isotherms of Cu^{2+} on different materials.

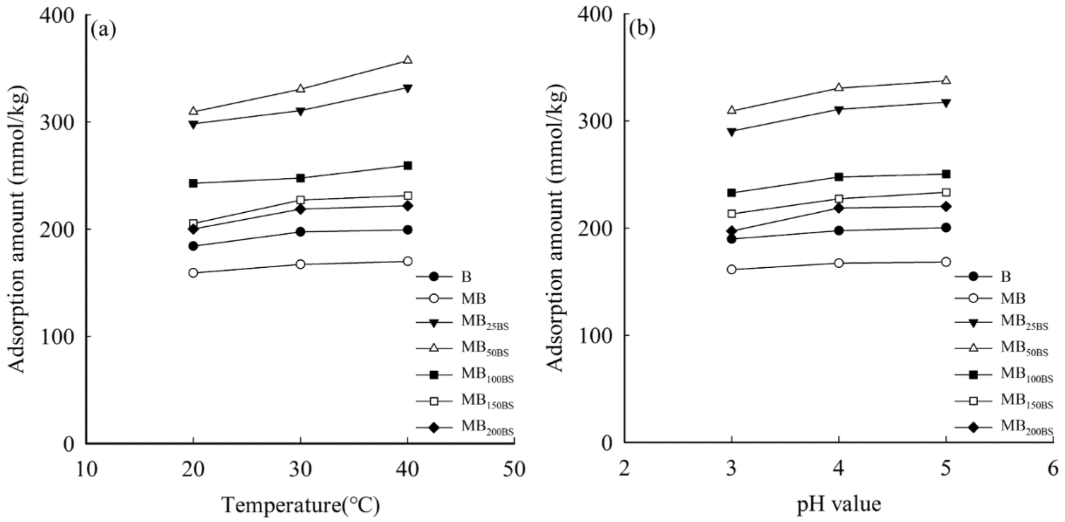

Fig. 4. (a) Temperature and (b) pH effect on Cu^{2+} adsorption by various materials.

Table 3
Cu^{2+} adsorption under different ionic strengths

Test materials	Adsorption amount of Cu^{2+} (mmol/kg)		
	I = 0.01 mol/L	I = 0.1 mol/L	I = 0.5 mol/L
B	200.24a ± 1.34	197.46a ± 0.65	190.25b ± 0.98
MB	170.11a ± 1.13	167.10ab ± 0.86	162.02b ± 0.79
MB_{25BS}	316.22a ± 1.01	310.70b ± 0.53	300.24c ± 1.02
MB_{50BS}	335.13a ± 0.14	330.55a ± 1.02	321.22b ± 1.06
MB_{100BS}	256.35a ± 0.75	247.74b ± 0.46	242.52b ± 1.33
MB_{150BS}	236.89a ± 0.88	227.23b ± 0.95	213.33c ± 0.79
MB_{200BS}	220.54a ± 0.70	218.76a ± 0.42	198.81b ± 0.34

The different lowercase letters indicate significant difference among treatments at 0.05 levels.

Table 4
Thermodynamic parameters of Cu^{2+} adsorption on different materials

Test materials	20°C			40°C		
	$\Delta G°$/(kJ/mol)	$\Delta H°$/(kJ/mol)	$\Delta S°$/[J/(mol K)]	$\Delta G°$/(kJ/mol)	$\Delta H°$/(kJ/mol)	$\Delta S°$/[J/(mol K)]
B	–13.97	3.01	57.92	–14.16	3.01	57.92
MB	–13.46	2.50	54.44	–13.62	2.50	54.44
MB_{25BS}	–14.19	4.09	62.35	–14.45	4.09	62.35
MB_{50BS}	–13.64	5.47	65.19	–13.99	5.47	65.19
MB_{100BS}	–13.80	2.50	55.60	–13.96	2.50	55.60
MB_{150BS}	–14.22	4.54	64.02	–14.51	4.54	64.02
MB_{200BS}	–14.07	3.94	61.42	–14.32	3.94	61.42

MB_{25BS} and MB_{200BS} increased by 9.29% and 11.71%, respectively, whereas the increase of 4.33%–5.63% in B and MB was mainly due to the competitive adsorption of H^+ and Cu^{2+} at low pH. Competitive adsorption gradually weakened with the increase in pH. In addition, the increase in pH caused the protonation of the B surface, which enhanced the adsorption amount of Cu^{2+} on different materials.

3.4. Effect of ionic strength on adsorption of Cu^{2+} on test materials

Table 3 shows that the adsorption amount of Cu^{2+} by each material decreased with the increase in ionic strength at the range of 0.01–0.5 mol/L, and the decrease ranged from 4.15% to 9.95%. The decrease in ranges followed the order MB_{150BS} (9.95%) > MB_{200BS} (9.85%) > MB_{100BS} (5.39%) > MB_{25BS} (5.05%) > MB (4.99%) > B (4.76%) > MB_{50BS} (4.15%). Under the treatment of I = 0.01 and 0.5 mol/L, the amount of Cu^{2+} adsorbed by each material was considerably differed because the increase in ionic strength could reduce the activity of Cu^{2+} in solutions, and Na^+ and Cu^{2+} in background solution exhibit competitive adsorption on the material surface [28].

3.5. Thermodynamic characteristics of Cu^{2+} adsorption

The thermodynamic parameters of Cu^{2+} on different materials (Table 4) show that the apparent free energy changes ($\Delta G°$) of Cu^{2+} adsorbed by each material were less than 0 at 20°C and 40°C, indicating that the adsorption was spontaneous. Under the same treatment, Cu^{2+} adsorption was more spontaneous at 40°C. The enthalpy change $\Delta H°$ of Cu^{2+} adsorption of each material was greater than zero, indicating that the reaction process was endothermic, which is consistent with the temperature effect in Fig. 2. The adsorption entropy $\Delta S°$ of Cu^{2+} was larger than zero, indicating that the adsorption process was an entropy-adding reaction. The adsorption disorder of MB_{50BS} was the largest, indicating that the adsorption of Cu^{2+} by MB_{50BS} was affected by B and BS-12.

4. Conclusion

- The B surface became rough after being loaded by Fe_3O_4, but the roughness of MB decreased after being modified by BS-12. The pH, CEC, and specific surface area of MB_{BS}s decreased with the increase in BS-12 modification ratio.
- Adsorption isotherms of Cu^{2+} on all tested materials were L-shaped and agreed with the Langmuir model. At the same equilibrium concentration, MB_{50BS} showed the strongest adsorption capacity for Cu^{2+} with the maximum adsorption capacity of 542.46 mmol/kg.
- The adsorption amount of Cu^{2+} on each material increased with the increase in temperature and pH, but decreased with the increasing ionic strength.
- The adsorption of Cu^{2+} by MB_{BS}s was a spontaneous, endothermic and entropy-adding process.

Acknowledgments

The authors wish to acknowledge and thank the Fundamental Research Funds of China West Normal University (17E057), the Scientific Research Foundation of the Education Department of Sichuan province (18ZB0576) and the financial assistance of Sichuan Science and Technology Program (2018JY0224).

References

[1] Q. Cai, M.L. Long, M. Zhu, Q.Z. Zhou, L. Zhang, J. Liu, Food chain transfer of cadmium and lead to cattle in a lead-zinc smelter in Guizhou, China, Environ. Pollut., 157 (2009) 3078–3082.

[2] R.H. Guo, H.M. Jin, H.S, Wu, H.Y. Huang, X.M. Yie, Y.D. Xu, M.J. Zheng, Total content of heavy metals and their chemical form changes in multilevel wastewater treatment system in intensive swine farm, Trans. Chin. Soc. Agric. Eng., 34 (2018) 210–216.

[3] X.L. Liu, R. Ma, X.X. Wang, Y. Ma, Y.P. Yang, L. Zhuang, S. Zhang, R. Jehen, J.R. Chen, X.K. Wang, Graphene oxide-based materials for efficient removal of heavy metal ions from aqueous solution: a review, Environ. Pollut., 252 (2019) 62–73.

[4] Z.Y. Zhou, Y.S. Liu, Preparation of non-sintered ceramsite from coal fly ash and its performance on heavy metals removal, Chin. J. Environ. Eng., 7 (2013) 4054–4060.

[5] S. Bai, Agricultural and forestry wastes material as potential adsorbent for heavy metal ions from aqueous solutions: a review, Environ. Sci. Technol., 37 (2014) 94–98.

[6] W.B. Li, Z.F. Meng, Z. Liu, Q. Wu, S.E. Xu, J. Zhu, Enhanced absorption of Cr(VI) on Lou soil by amphoteric and amphoteric cationic modified bentonite, J. Environ. Sci. China, 36 (2016) 3810–3817.

[7] Y.Q. Wu, C. Xu, Y. Zhao, Q. Yan, Preparation of calcium silicate-chitosan polymer and the adsorptive removal of heavy metals in wastewater, Environ. Chem., 35 (2016) 562–567.

[8] H.W. Pang, Y.H. Wu, X.X. Wang, B.W. Hu, X.K. Wang, Recent advances in composites of graphene and layered double hydroxides for water remediation: a review, Chem. Asian J., 14 (2019) 2542–2552.

[9] Y. Wu, G. Xu, Y.C. Lv, H.B. Shao, Effects of biochar amendment on soil physical and chemical properties: current status and knowledge gaps, Adv. Earth Sci., 29 (2014) 68–79.

[10] H.H. Lv, Y.Y. Gong, J.C. Tang, Y. Huang, K. Gao, Advances in preparation and applications of biochar and its composites, J. Agro-Environ. Sci., 34 (2015) 1429–1440.

[11] B.P. Singh, B.J. Hatton, B. Singh, A.L. Cowie, A. Kathuria, Influence of biochars on nitrous oxide emission and nitrogen leaching from two contrasting soils, J. Environ. Qual., 39 (2010) 1224–1235.

[12] Y.L. Ding, J. Liu, Y.Y. Wang, Effects of biochar on microbial ecology in agriculture soil: a review, Chin. J. Appl. Ecol., 24 (2013) 3311–3317.

[13] X.Y. Lin, Y.D. Jing, C. Gong, Z.L. He, Research progress on the sorption of heavy metals by biochar, Environ. Pollut. Control, 36 (2014) 83–87.

[14] W.F. Chen, W.M. Zhang, J. Meng, Biochar and agro-ecological environment: review and prospect, J. Agro-Environ. Sci., 33 (2014) 821–828.

[15] C.R. Xie, Z.W. Wang, J.M. Zhu, J.H. Gao, H.Y. Zhang, X.Y. Xie, C. Jin, Adsorption of lead and copper from aqueous solutions on biochar produced from walnut green husk, Acta Sci. Circumstantiae, 36 (2016) 1190–1198.

[16] H.Y. Ji, Y.Y. Wang, H.H. Lv, Y.X. Liu, R.Q. Yang, S.M. Yang, Cadmium adsorption by biochar prepared from pyrolysis of silk waste at different temperatures, Chin. J. Appl. Ecol., 29 (2018) 1328–1338.

[17] M.S. Wu, J.F. Ma, S.M. Yang, G.L. Tian, Y.H. Wang, X.E. Liu, Progress of the magnetic biochar composite materials, Funct. Mater., 47 (2016) 7028–7033.

[18] X. Wan, C.G. Mei, L.Z. He, Y.L. He, J.G. Yuan, C.D. Wang, On the synthesis, characterization and phosphate removal of the biocharbased magnetic composites, J. Saf. Environ., 17 (2017) 1069–1075.

[19] W.Q. Du, W. Cao, H. Zhou, W.T. Yang, J.F. Gu, P.Q. Peng, P. Zhang, B.H. Liao, Optimization and the mechanismin treatment of heavy metals wastewater with magnetic biochar, Acta Sci. Circumstantiae, 38 (2018) 492–500.

[20] B.Y. Mo, Y.B. Tang, F.Y. Chen, T. Wen, Preparation of magnetic activated carbon granules for adsorption of methyl orange in water, Chin. J. Environ. Eng., 9 (2015) 1863–1868.

[21] M.M. Zhang, Y.G. Liu, T.T. Li, W.H. Xu, B.H. Zheng, X.F. Tan, H. Wang, Y.M. Guo, F.Y. Guo, S.F. Wang, Chitosan modification of magnetic biochar produced from *Eichhornia crassipes* for enhanced sorption of Cr(VI) from aqueous solution, RSC Adv., 5 (2015) 46955–46964.

[22] X.H. Zhou, J.J. Zhou, Y.C. Liu, J. Guo, J.L. Ren, F. Zhou, Preparation of iminodiacetic acid-modified magnetic biochar by carbonization, magnetization and functional modification for Cd(II) removal in water, Fuel, 233 (2018) 469–479.

[23] S.X. Dong, J.X. He, M. Li, Research on the properties of eco-detergent BS-12 in reactive dye washing, Text. Aux., 24 (2007) 31–33.

[24] P.P. Zhao, Z.F. Meng, Y.T. Yang, S.Y. Yang, S. Ren, Q. Wu, B. Li, J.T. Wang, Studies on adsorption characteristics of BS-12 on kaolinite and its affecting factors, Chin. J. Soil Sci., 46 (2015) 1226–1231.

[25] Z.F. Meng, Y.P. Zhang, G.D. Wang, Sorption of heavy metal and organic pollutants on modified soils, Pedosphere, 17 (2007) 235–245.

[26] S. Ren, Z.F. Meng, W. Liu, W.B. Li, J. Deng, Characterization and adsorption performance of phenol on amphoteric modified magnetic bentonites, J. Agro-Environ. Sci., 36 (2017) 108–115.

[27] W.B. Li, Z.F. Meng, Z. Liu, H.Y. Chen, Q. Wu, S.E. Xu, Chromium (VI) adsorption characteristics of bentonite under different modification patterns, Pol. J. Environ. Stud., 25 (2016) 1075–1083.

[28] T. Xie, W.B. Li, Z.F. Meng, H.Y. Lu, S. Ren, S. Yek, Studies on Cr(VI) and Cd^{2+} adsorption onto bentonite modified by a BS-12+DTAB complex, J. Agro-Environ. Sci., 36 (2017) 1778–1786.

[29] T. Wang, Z.F. Meng, S. Ren, Y. Zhang, W. Liu, W.B. Li, K. Tian, Differences between phenol and phenanthrene adsorption on BS-12/DTAB combined modified bentonite, Acta Sci. Circumstantiae, 37 (2017) 3951–3958.

[30] S. Ren, Z.F. Meng, X.X. Sun, H.Y. Lu, M.F. Zhang, A.H. Lahori, S.B. Bu, Comparison of Cd^{2+} adsorption onto amphoteric, amphoteric-cationic and amphoteric-anionic modified magnetic bentonites, Chemosphere, 239 (2020) 124840–124848.